MAGNETIC RESONANCE IN MEDICINE 5, 99–108 (1987)

The Design of a Multiple Inversion Recovery Sequence for T1 Measurement

I. R. YOUNG,*† A. S. HALL,* AND G. M. BYDDER‡

*GEC Research Limited, Hirst Research Centre, East Lane, Wembley, Middlesex HA9 7PP, United Kingdom; and ‡NMR Unit, Hammersmith Hospital, Ducane Road, London W12 4RS

Received October 31, 1986; revised February 13, 1987

Inversion recovery has the potential to be a powerful method of determining the values of T1 in *in vivo* studies. However, because of its relative slowness it is not practical to undertake several experiments with different values of the interval between the magnetization inverting 180° pulse and the interrogating 90° one. The multiple inversion recovery method described here uses a series of sampling pulses, most much less than 90°, to produce a series of images. It is shown that slice shape is relatively reproducible from one sample to another and that, largely as a result, the accuracy of the sequence in measuring T1 is encouraging.

1. INTRODUCTION

Inversion recovery is a relatively slow method of imaging, so that in spite of its very high contrast, doubts about its efficiency have been expressed (*1*). However, because of its sensitivity to differences in T1 and because of its independence of slice shape artifacts of various kinds (*2*), it can be used to produce reliable measurements of T1 (*3*, *4*).

This paper describes results obtained by sampling the magnetization recovery curve several times, with precession angles reduced (except for the last one) well below 90°, thus allowing some magnetization to remain along the z-axis and to be available for subsequent sampling (a technique first proposed in nonimaging terms some years ago (*5*)). The method is readily practical in a typical imager, using standard multiecho software, so that the questions to be resolved are, on the one hand, its freedom from artifact and, on the other, its ability to provide at least one or two images from the set acquired which are acceptable for clinical diagnosis (so avoiding the need to obtain additional images for this purpose).

It is shown that contrast and relative image quality can be readily manipulated and that the method results in accurately repeatable slice shapes. On the other hand, signal amplitudes are hard to predict unless the slice shape is perfect. Measurement is best made by determining the value of the interval between the 180 and 90° pulses of which the magnetization of a region is zero, meaning that true reconstruction of the images (retaining the sign of the magnetization (*6*, *7*)) is to be preferred, rather than magnitude reconstruction (*8*).

† To whom correspondence should be addressed.

0740-3194/87 $3.00

Results from the procedure suggest that it is capable of providing useful T1 measurements from a single set of images.

2. THEORETICAL BACKGROUND

1. Basic Relations

Although, in theory, any number of interrogations could be attempted, the number used in this study is four. Unlike the case with sequences designed for the multiple refocusing of spins (such as the Carr–Purcell–Meiboom–Gill sequence (*9*)), following a spin inversion, inverted magnetization is, in effect, "used up" by multiple interrogations, so that increasing their number is possible only with some loss of individual quality.

For simplicity the interval between interrogations is assumed to be the same in all cases and is called tI. While this restriction is not necessary, it makes the iterations needed to obtain numerical values much easier. The time between the last interrogating pulse and the next inverting pulse is called tx. The four interrogating precession angles are A, B, C, D (all $>0°$, $\leq 90°$) as shown in Fig. 1 which presents the sequence used.

Then using the notation

$$\mathrm{cA} = \cos A, \qquad \mathrm{sA} = \sin A, \qquad \mathrm{cB} = \cos B, \qquad \text{and so on, and}$$

$$\mathrm{Ex} = \exp(-\mathrm{tx}/\mathrm{T1}), \qquad E_\mathrm{I} = \exp(-\mathrm{tI}/\mathrm{T1}), \qquad \mathrm{Et} = \exp(-\mathrm{tE}/\mathrm{T2}),$$

the signals (S(I) to S(IV)) for the four interrogations can be obtained by simple manipulation and are given by

$$S(\mathrm{I}) = S_0\mathrm{EtsA}(1 - E_\mathrm{I}(2 - \mathrm{Ex})) \qquad [1]$$

$$S(\mathrm{II}) = S_0\mathrm{EtsB}(1 - E_\mathrm{I}(1 - \mathrm{cA}) - \mathrm{cA}E_\mathrm{I}^2(2 - \mathrm{Ex})) \qquad [2]$$

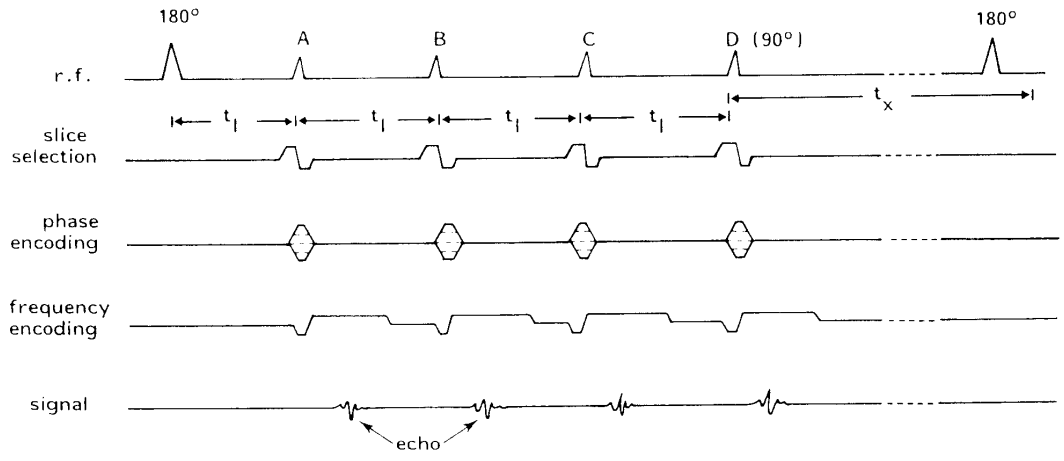

FIG. 1. Sequence used in the multiple inversion recovery sequence analysis. The form of data acquisition used is a field echo, but a spin-echo method is also possible. By using a multiple spin echo following the last interrogation, T2 information can be obtained at the same time as T1.

$$S(\mathrm{III}) = S_0\mathrm{EtsC}(1 - E_\mathrm{I}(1 - \mathrm{cB}) - \mathrm{cB}E_\mathrm{I}^2(1 - \mathrm{cA}) - \mathrm{cBcA}E_\mathrm{I}^3(2 - \mathrm{Ex})) \quad [3]$$

$$S(\mathrm{IV}) = S_0\mathrm{EtsD}(1 - E_\mathrm{I}(1 - \mathrm{cC}) - \mathrm{cC}E_\mathrm{I}^2(1 - \mathrm{cB}) - \mathrm{cBcC}E_\mathrm{I}^2(1 - \mathrm{cA}) - \mathrm{cCcBcA}E_\mathrm{I}^4(2 - \mathrm{Ex})). \quad [4]$$

These relations assume perfect rectangularly shaped slices, and, as a result, signals can be significantly different from those predicted in practice as will be discussed. S_0 is the available fully relaxed signal, and tE is the time to the echo during data acquisition.

Because the sequence can be designed so that samples are taken at times straddling those for which the signals from any likely tissue of interest may be expected to be zero, the simplest strategy in taking measurements from the relatively small number of images which can be obtained in a typical whole-body experiment is to plot the signal amplitudes for the four images and to determine the times at which the signals from the various tissues are zero. At these times, the following various relations hold:

(a) between inversion and the first interrogation

$$2\mathrm{E0} = (1 + \mathrm{Ex}), \quad [5]$$

where E0 = exp(−t0/T1) where t0 is the time at which the signal from a region is determined to be zero.

(b) Between the first and second interrogations

$$1 - \mathrm{E}(0 - \mathrm{I})(1 - \mathrm{cA}) = \mathrm{cAE0}(2 - \mathrm{Ex}), \quad [6]$$

where E(0 − I) = exp(−(t0 − tI))/T1.

(c) Between the second and third interrogations

$$1 - \mathrm{E}(0 - 2\mathrm{I})(1 - \mathrm{cB}) - \mathrm{cBE}(0 - \mathrm{I})(1 - \mathrm{cA}) = \mathrm{cAcBE0}(2 - \mathrm{Ex}), \quad [7]$$

where E(0 − 2I) = exp(−(t0 − 2tI))/T1).

(d) Between the third and fourth interrogations

$$1 - \mathrm{E}(0 - 3\mathrm{I})(1 - \mathrm{cC}) - \mathrm{cCE}(0 - 2\mathrm{I})(1 - \mathrm{cB}) - \mathrm{cCcBE}(0 - \mathrm{I})(1 - \mathrm{cA}) = \mathrm{cAcBcCE0}(2 - \mathrm{Ex}), \quad [8]$$

where $E(0 - 3\mathrm{I})$ = exp(−(t0 − 3tI))/T1).

In principle, there is no reason why the crossover point for the signal from a tissue should not be at times greater than 4tI, but it would seem to be a better strategy to design the sequences so that there is at least one sample on each side of the zero signal from a tissue, rather than extrapolating from the set of four.

Apart from the first, these relations are best evaluated for the values of t_0 found by selecting a probable value for T1 and improving the estimate by iteration until satisfactory accuracy is achieved. If A is small, $\cos A \approx 1$ and Eq. 6 can be simplified to

$$1 = \mathrm{cAE0}(2 - \mathrm{Ex}). \quad [9]$$

If B is also relatively small, an adequate first estimate for the T1 of a tissue with zero signal between the second and third interrogations is

$$1 = \mathrm{cAcBE0}(2 - \mathrm{Ex}). \quad [10]$$

2. *Contrast and Signal*

Evaluation of relations [1] to [4] shows that the sequence designer has several options available in deciding what sort of balance to aim for in the set of four images. The two primary factors which are available for adjustment are tI and the four precession angles *A*, *B*, *C*, and *D*. The maximum length of 4tI (the timing of the last interrogation) is determined by the T1 value of the tissues from which measurable contrast is sought in the last image. In imaging the adult brain at 0.15 T (with a T1 of gray matter of perhaps 500–550 ms and that of white matter of 350–400 ms) we find a value of tI of 120 ms to be useful.

There is no value in making angle *D* anything other than 90° so as to use any magnetization which is left, although (as will be suggested in the next section) this can cause problems with relative signal amplitudes. Apart from that, the choice of how to apply the available magnetization is a matter for the user. If one or two very high quality images are needed for diagnostic purposes, then the magnetization must be concentrated in them. If constant contrast over the set is the target, then a different set of angles is appropriate.

Table 1 shows the predicted signals and contrasts (signal differences) for gray and white matter, calculated using the parameters given in the legend, for two sets of precession angles. The first, with angles of 14.5, 19, 30, and 90°, was designed to give one very high quality image, together with enough performance in the other images to enable T1 to be measured. In the second sequence, with precession angles of 27, 45, 45, and 90°, the aim was to produce constant contrast in the four images.

3. *Artifacts*

One advantage of measurements using inversion recovery systems, reported earlier (*2*), is their relative independence of artifacts such as those due to slice shape. If accurate

TABLE 1

Signals and Contrast for Gray and White Matter

	Set of angles (14.5, 19, 30, 90°)			Set of angles (27, 45, 45, 90°)		
Image no.	WM[a] signal	GM[b] signal	Contrast (W–G)	WM signal	GM signal	Contrast (W–G)
I	−0.07	−0.09	0.02	−0.10	−0.14	0.04
II	0	−0.04	0.04	0	−0.04	0.04
III	0.09	0.04	0.05	0.11	0.06	0.05
IV	0.30	0.21	0.09	0.23	0.19	0.04

Note. Signal and contrast for gray and white matter calculated for two multiple IR sequences both with values of tI of 120 mm, but the first (sequence A) with precession angles of 14.5, 19, 30, and 90° and the second (sequence B) with angles of 27, 45, 45, and 90°. Contrast figures are simply the signal differences. All signals are normalized to that from gray matter using a partial saturation sequence with tR = 5T1 and very short tE. Tissue parameters used were the following. Gray matter: T1 = 500 ms, T2 = 95 ms, and relative proton density = 1. White matter: T1 = 380 ms, T2 = 85 ms, and relative proton density = 0.9.

[a] WM = white matter.

[b] GM = gray matter.

measurements are to be attempted, it is necessary that the system be as free from artifact as possible and that those which do arise shall be marginal or correctable. Some experimental results are quoted in this section for convenience, preceding the main results section, but were derived as described under Results.

The forms of the slices for the four interrogations using the 14.5, 19, 30, and 90° series measured experimentally are shown in Fig. 2. The results were obtained by determining the amplitudes of signals from a phantom having a slot containing doped water at an angle of 45° to the central plane of the slice. The profiles are offset in the drawing (by approximately 10% of their amplitude relative to each other) since they would otherwise overlap too closely to show differences of detail clearly. In Table 2 the percentages of total signal obtained from the four slices within the limits at which the signals are 10% of their peak amplitude are indicated.

These results show that the slice is highly reproducible with this method. Using a sequence differing only in that the inverting 180° pulse is omitted, it is, however, apparent that the relative amplitudes of the signals can be significantly different from those predicted and that calibration is necessary. This is illustrated in Table 3, which records the predicted signals and those actually measured for the same tI of 120 ms

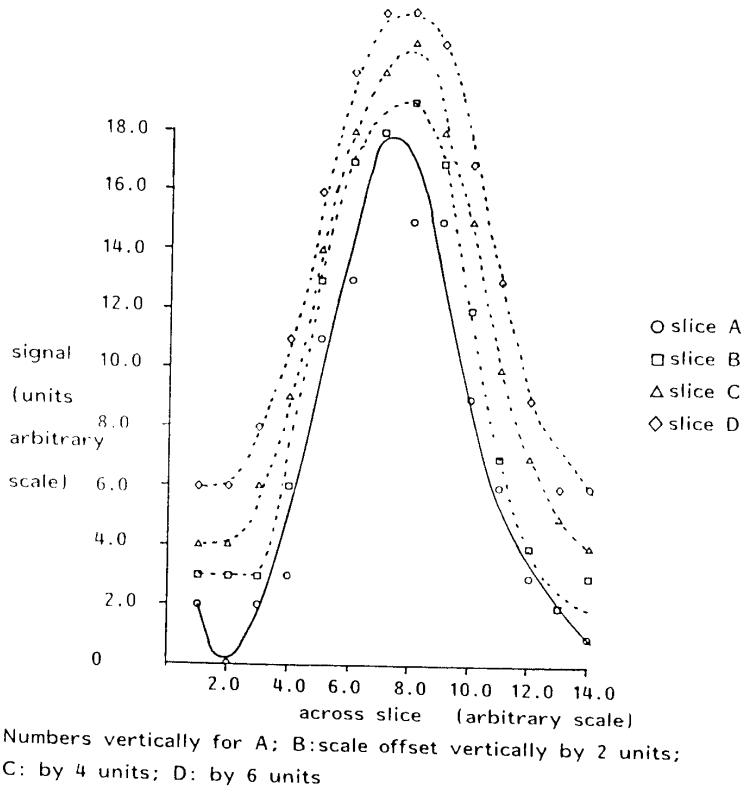

FIG. 2. Slice shapes measured for the four images in a 14.5, 19, 30, and 90° set. The slices were measured by recording the amplitudes of signals from an offset pair of wedges in a phantom forming a water-filled slot at 45° to the plane of the slices. When measured all were normalized to have the same peak amplitude, but are presented offset from each other so as to make the similarities and differences between them more obvious.

TABLE 2

Slice Signal Consistency

Image no.	Percentage within 10% limits
I	87.0
II	89.0
III	88.6
IV	89.5

Note. Table indicating the consistency of the slices in a multiple inversion recovery set. The values are the percentages of total signal (to a distance of twice nominal slice width) contained within the lines at which signal amplitude is 10% of that of the maximum.

using the set of angles giving uniform contrast. The predicted signals were given by the following (using the same notation as before),

$$\text{for slice I} \qquad S(\mathrm{I}) = S_0\mathrm{EtsA}(1-\mathrm{Ex}) \qquad [11]$$

$$\text{for slice II} \qquad S(\mathrm{II}) = S_0\mathrm{EtsB}(1-E_\mathrm{I}+\mathrm{cA}E_\mathrm{I}(1-\mathrm{Ex})) \qquad [12]$$

$$\text{for slice III} \qquad S(\mathrm{III}) = S_0\mathrm{EtsC}(1-E_\mathrm{I}+\mathrm{cB}E_\mathrm{I}(1-E_\mathrm{I})+\mathrm{cAcB}E_\mathrm{I}^2(1-\mathrm{Ex}) \qquad [13]$$

TABLE 3

Calibration Values

Image no.	Measured amplitudes	Rectangular slice	Triangular slice
I	0.30	0.66	0.45
II	0.58	0.98	0.69
III	0.54	0.80	0.63
IV	1.0	1.0	1.0

Note. Measurements and theoretical predictions from the relations in Eqs. [11] to [14] using the modified multiple inversion recovery sequence described in the text. The results of a practical experiment are given in the left-hand column and those predicted from rectangular and triangular slices are in the other two columns. In each case the set of signals was normalized to that from the 90° pulse. Precession angles used were 27, 45, 45, and 90° as this formed the sequence which might be expected to give more consistent results of the pair being analyzed. The triangular slice predictions were made by integrating the values determined from calculating the amplitudes of eight sections on either side of the center of the slice. The precession angles assumed for each section were varied linearly from the center (for which the value given was used) to the edge.

for slice IV $$S(\mathrm{IV}) = S_0\mathrm{EtsD}(1 - E_\mathrm{I} + \mathrm{cC}E_\mathrm{I}(1 - E_\mathrm{I}) + \mathrm{cBcC}E_\mathrm{I}^2(1 - E_\mathrm{I}) + \mathrm{cAcBcC}E_\mathrm{I}^3(1 - \mathrm{Ex})), \quad [14]$$

where the time interval between interrogations is still called tI, and tx is the time between the last pulse (with precession angle D) of one set and the first of the next.

The match between theoretical and actual results is poor and explained largely by problems with slice shape. As the last column of the table, which is plotted (as defined in the table legend) on the assumption that instead of being rectangular the slice is triangular, shows, there are substantial differences in the predicted signals. There is a relative enhancement of the signals for slices with bigger precession angles due to contributions from the sloping sides. The effects of these are emphasized to a significant extent in the table because a material with a long T1 (1500 ms) was chosen for the calibration to emphasize the point. In practice, the method used is to calibrate the system using the multiple inversion recovery sequence, but with a phantom-containing material with well-characterized T1 values in the expected range in the *in vivo* experiments.

3. RESULTS

All the practical work was performed on the Picker prototype NMR imager installed at Hammersmith Hospital (*10*) which operates at 0.15 T. Due to limitations of its computer storage capacity, this machine can only acquire four low-resolution (128 × 128) images when used in multislice mode, as in this study. All the images were acquired with a nominal slice width (within limits defined by 10% of the peak amplitude) of between 4 and 5 mm.

All phantom and test data were acquired using a single pass (128 projections) while the head and peripheral images were the result of four repetitions (512 projections). tR was 1480 ms (as defined by the American College of Radiology glossary (*11*)), with a tI of 120 ms, and a period (tx) between the last interrogating pulse and the next 180° pulse of 1000 ms.

Apart from the slice calibration material in the previous section, images of a series of bottles containing water doped with Gd-DTPA (*12*) were acquired to give a range

TABLE 4

Measured Values of T1 in Phantoms

Value measured by multiple IR (ms)	Value measured by PS and IR (ms)
150	134
213	202
315	345
608	648
(Mean estimated errors = 27 ms)	(Mean estimated errors = 23 ms)

Note. Comparison of measurements on a phantom of gadolinium–DTPA-doped water made with the multiple IR and a pair of PS and IR sequences.

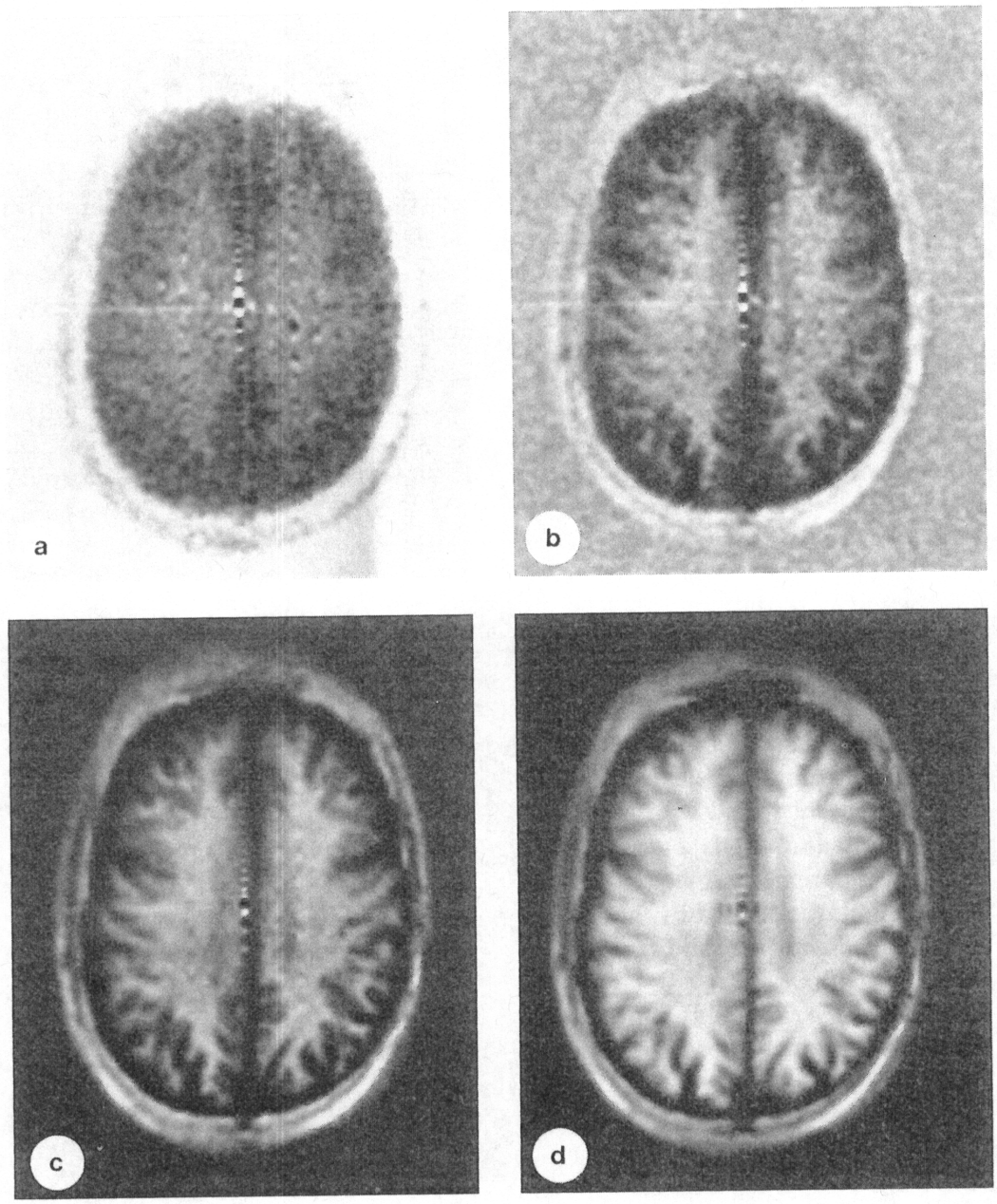

FIG. 3. Set of images with a matrix of 128 × 128 (slice thickness 4.5 mm, approximately) taken using the multiple IR sequence with precession angles of 14.5, 19, 30, and 90°, with 512 projections. Reconstruction was true (5) (with the gray scale centered on the zero signal level and both negative and positive values appearing in the images). A calibration sequence using the same precession angles without the inverting pulse was used to obtain the reference phase matrix for the true reconstruction. (a) 14.5°, (b) 19°, (c) 30°, (d) 90°.

of values of T1. Measurements were taken from the bottles and Eqs. [5] to [8] were used to derive values for T1. These are shown in Table 4 compared with the results of imaging the same bottles using a partial saturation sequence with a tR of 1500 ms

and an inversion recovery sequence with a tR of 1500 ms and tI of 500 ms. tE was the same in all cases. The mean estimated errors in the readings are given, and it is seen that the match between the two sets of results is adequate.

Figures 3a to 3d form a set of images obtained with the 14.5, 19, 30, and 90° set of precession angles, intended to optimize the final image for diagnostic purposes. Measurements of four points on the images for white matter and two on gray matter gave 365 ± 10 and 545 ± 13 ms respectively for the T1 values for the two tissues. These compare with values obtained from the same volunteer's head at the same locations using the IR and PS sequences of 380 ± 25 and 520 ± 18 ms. Leg muscle gave a T1 of 260 ± 15 ms in another test, which compares well with other previous results, but the measurement of fat (125 ± 17 ms) was significantly lower than expected (although, unlike the other tissues, the value of t_0 had to be obtained by extrapolation, as its signal was not negative in any image). In this latter study no alternative measurements were recorded at the time of the experiment.

4. DISCUSSION

The multiple inversion recovery method appears to have the potential of obtaining T1 information from a single scan, in much the same way that T2 data can be extracted from a multiple echo sequence (*13*). In the form of back projection in which data are acquired from the decaying FID immediately after slice selection (*10*), images formed only from real data can be produced, in which the sign of the magnetization is retained. In this case, the multiple inversion recovery method allows the determination of T1 from a single sequence. In 2D Fourier transform imaging using the standard spin warp method (*14*), it is necessary to use a second set of data to provide a reference set of phase data (*6*, *7*). This can be acquired using short tR and low resolution.

Intuitively, it seems to be an attractive approach to make measurements by seeking the times at which signals are zero, since this eliminates many of the potential doubts about the accuracy of amplitudes measured in the system. Curve-fitting methods have been found to be preferable to crossing techniques in previous work (*15*), but the number of points for fitting that can be obtained in a typical examination time is usually relatively small, and the optimum strategy in whole-body MRI may well be different.

5. CONCLUSIONS

The multiple inversion recovery approach to the measurement of T1 seems to justify further exploration, for it is both convenient to implement and swift in its operation.

ACKNOWLEDGMENTS

We acknowledge the continuing support of the Medical Research Council and the Department of Health and Social Security (and especially Mr. G. R. Higson and Mr. J. L. Williams) in the evaluation of the clinical usefulness of MRI of which this work forms part.

REFERENCES

1. W. A. EDELSTEIN, P. A. BOTTOMLEY, H. R. HART, AND L. S. SMITH, *J. Comput. Assist. Tomogr.* 7, 391 (1983).

2. I. R. YOUNG, D. J. BRYANT, AND J. A. PAYNE, *Magn. Reson. Med.* **2,** 335 (1985).
3. C. J. HARDY, W. A. EDELSTEIN, D. VATIS, R. HARMS, AND W. J. ADAMS, *Magn. Reson. Imaging* **3**(2), 107 (1985).
4. M. A. LIN, *Magn. Reson. Med.* **2**(3), 234 (1985).
5. R. KAPTEIN, K. DIJKSTRA, AND C. E. TARR, *J. Magn. Reson.* **24,** 295 (1976).
6. I. R. YOUNG, D. R. BAILES, AND G. M. BYDDER, *Magn. Reson. Med.* **2,** 81 (1985).
7. H. W. PARK, M. H. CHO, AND Z. H. CHO, *Magn. Reson. Med.* **3**(1), 15 (1986).
8. R. GRAUMANN, M. DEIMLING, T. HEILMANN, AND A. OPPELT, "Proceedings, 5th Ann. Mtg. Soc. Mag. Res. Med., Montreal," pp. 922–923, 1986.
9. S. MEIBOOM AND D. GILL, *Rev. Sci. Instrum.* **29,** 688 (1958).
10. I. R. YOUNG, D. R. BAILES, M. BURL, A. G. COLLINS, D. T. SMITH, M. MCDONNELL, J. S. ORR, L. M. BANKS, G. M. BYDDER, R. H. GREENSPAN, AND R. E. STEINER, *J. Comput. Assist. Tomogr.* **6,** 1 (1982).
11. "American College of Radiology Glossary of NMR Terms," ACR, Chicago, 1983.
12. H. J. WEINMANN, R. C. BRASCH, W. R. PRESS, AND G. E. WESBEY, *AJR* **142,** 619 (1984).
13. L. E. CROOKS, M. ARAKAWA, J. C. HOENNINGIS, J. WATTS, R. MCREE, L. KAUFMAN, P. L. DAVIES, A. R. MARGULIS, AND J. DEGROOT, *Radiology* **143,** 169 (1982).
14. J. M. S. HUTCHISON, W. A. EDELSTEIN, AND E. JOHNSON, *J. Phys. E* **13,** (1980).
15. T. K. LEIPERT AND D. W. MARGUARDT, *J. Magn. Reson.* **24,** 181 (1976).